Attenuation Correction of a Simple Phantom from Simultaneous SPECT and MR Imaging

M. J. Hamamura[1], S. Ha[1], W. W. Roeck[1], L. T. Muftuler[1], D. J. Wagenaar[2], D. Meier[2], B. E. Patt[2], and O. Nalcioglu[1]
[1]Tu & Yuen Center for Functional Onco-Imaging, University of California, Irvine, CA, United States, [2]Gamma Medica-Ideas, Inc., Northridge, CA, United States

Purpose

Accurate SPECT imaging requires correction for the attenuation of the gamma rays by the object. Determination of an accurate, object-specific attenuation map is required to perform such an attenuation correction (AC). Strategies for obtaining this attenuation map include 1) importing and registering the map derived from another modality, 2) acquiring transmission data for estimating the map using an external source, and 3) estimating the map solely from the emission data. For this study, we utilized the first method through the simultaneous acquisition of MRI and SPECT data by a novel MR-SPECT imaging system. Simultaneous acquisition of these data allows for exact co-registration of the MRI-based attenuation map and the nuclear projection data, and eliminates the extra time required for 2 sequential scans.

Methods

The test phantom consisted of a hollow acrylic cylinder (outer diameter = 22 mm, inner diameter = 19 mm) containing several acrylic rods (diameter = 3 mm) and filled with a ^{99m}Tc / $CuSO_4$ solution (Fig 1a). The phantom was placed in the center of a custom RF birdcage coil in which the separation between two rungs was opened to allow for the insertion of a lead parallel-hole collimator. The collimator was positioned next to a cadmium-zinc-telluride (CZT) nuclear radiation detector unit on one end, and fixed 1 cm from the test phantom on the opposite end. The CZT detector measures 2.54 x 2.54 x 0.5 cm and consists of 16 x 16 pixels (1.59 mm pitch). The CZT detector/RF coil/phantom setup was placed into a 4 T MRI system, as diagramed in Fig. 2.

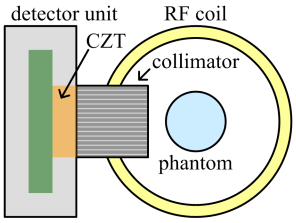

Fig. 2. *MR-SPECT setup*

For each of 30 views about the phantom (12 degree steps) an MR image was acquired using a 2D spin-echo pulse sequence with the following parameters: TR = 500 ms, TE = 20 ms, FOV = 40 mm, matrix = 128 x 128, slice thickness = 4 mm. 2D projection data were simultaneously acquired using a 10% energy window around the 140 keV photopeak. The contribution of each (radioactive) voxel to the projection data was attenuated by the product over N of $\exp(-\mu_N d_N)$, where μ_N is the linear attenuation coefficient of the N-th component (e.g. water, acrylic) and d_N is the distance across the N-th component region from the voxel to the detector. For each view, the co-registered MR image was used to define the different component regions and measure the d_N (Fig 1b). An AC factor was then calculated and applied to the projection data (Fig 1c).

For analysis, both corrected and uncorrected projection data were used in the SPECT reconstruction. Filtered-back-projection with the Hann filter was performed on these data, and the resulting reconstructed SPECT images were interpolated to the same FOV and matrix as the MR images for direct comparison (Fig 1d).

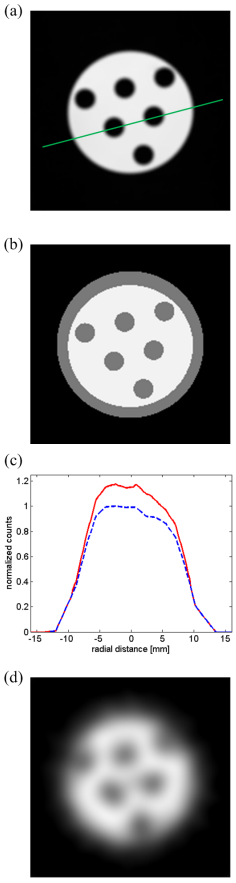

Fig. 1. *(a) MRI, (b) attenuation map (white = water, gray = acrylic) and (c) projection data profiles (blue = uncorrected, red = corrected) for one of the 30 views, and (d) the resulting AC SPECT image.*

Results

The MR image and the corresponding uncorrected nuclear projection data (blue) and AC projection data (red) are shown in Figs. 1a and 1c respectively. The SPECT reconstruction using the AC projection data is shown in Fig. 1d. Profiles along the green line in Fig. 1a of the MR image (black), uncorrected SPECT image (blue), and AC SPECT image (red) are shown in Fig. 3.

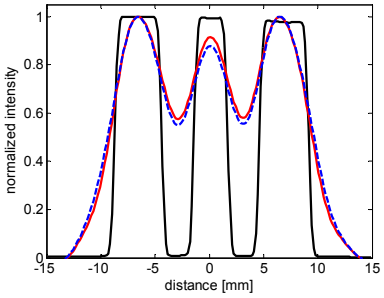

Fig. 3. *MR (black) and SPECT (blue = uncorrected, red = corrected) image profiles across the green line in Fig 1a.*

Discussion

As anticipated, object attenuation results in a reduction of the measured counts, as seen in Fig. 1c. As seen in Fig 3, AC of the projection data slightly sharpens the phantom boundary and reduces signal loss in the center region of the reconstructed SPECT image. While these effects for this small size phantom are subtle, their magnitude will increase when imaging larger objects (e.g. humans). Never the less, even for these small animal scales, gamma ray attenuation produces a measurable effect that degrades the quality of SPECT imaging for quantification. This study demonstrates the feasibility of utilizing simultaneously acquired MR images for AC in SPECT, which becomes more significant as MR-SPECT systems are scaled up for use in human studies.

For this study, we utilized a simple AC method appropriate for our (two-component) phantom. However, segmentation of the MRI of a more complex object can be used to generate a more complex attenuation map. Given this attenuation map, numerous established AC techniques can be applied to reconstruct the SPECT image of this complex object [i.e. Chang, IEEE Trans Nucl Sci 25:638-43 (1978)]. The primary motivation of this study was not to perform an in-depth analysis of AC methods, but to demonstrate the feasibility of performing AC using data acquired from simultaneous MR and SPECT imaging.

This research is supported in part by CIRM grant RT1-01120, CIRM training grant T1-00008 (for S. Ha) and NIH NIBIB grant R44EB006712.